THE JOURNAL OF BIOLOGICAL CHEMISTRY VOL. 286, NO. 8, pp. 6402–6413, February 25, 2011

New Alkaloid Antibiotics That Target the DNA Topoisomerase I of *Streptococcus pneumoniae*[*] [S]

Received for publication, May 26, 2010, and in revised form, December 15, 2010 Published, JBC Papers in Press, December 17, 2010, DOI 10.1074/jbc.M110.148148

María Teresa García[‡], María Amparo Blázquez[§], María José Ferrándiz[‡], María Jesús Sanz[§], Noella Silva-Martín[¶], Juan A. Hermoso[¶], and Adela G. de la Campa[‡1]

From the [‡]Unidad de Genética Bacteriana, Centro Nacional de Microbiología and CIBER Enfermedades Respiratorias, Instituto de Salud Carlos III, 28220 Majadahonda, Madrid, the [§]Departamento de Farmacología, Facultat de Farmàcia, Universitat de València, Vicent Andrés Estellés s/n. 46100 Burjasot, Valencia, and the [¶]Grupo de Cristalografía Macromolecular y Biología Estructural, Instituto de Química-Física "Rocasolano", CSIC, Serrano 119, 28006 Madrid, Spain

Streptococcus pneumoniae **has two type II DNA-topoisomerases (DNA-gyrase and DNA topoisomerase IV) and a single type I enzyme (DNA-topoisomerase I, TopA), as demonstrated here. Although fluoroquinolones target type II enzymes, antibiotics efficiently targeting TopA have not yet been reported. Eighteen alkaloids (seven aporphine and 11 phenanthrenes) were semisynthesized from boldine and used to test inhibition both of TopA activity and of cell growth. Two phenanthrenes (seconeolitsine and *N*-methyl-seconeolitsine) effectively inhibited both TopA activity and cell growth at equivalent concentrations (~17 μM). Evidence for *in vivo* TopA targeting by seconeolitsine was provided by the protection of growth inhibition in a *S. pneumoniae* culture in which the enzyme was overproduced. Additionally, hypernegative supercoiling was observed in an internal plasmid after drug treatment. Furthermore, a model of pneumococcal TopA was made based on the crystal structure of *Escherichia coli* TopA. Docking calculations indicated strong interactions of the alkaloids with the nucleotide-binding site in the closed protein conformation, which correlated with their inhibitory effect. Finally, although seconeolitsine and *N*-methyl-seconeolitsine inhibited TopA and bacterial growth, they did not affect human cell viability. Therefore, these new alkaloids can be envisaged as new therapeutic candidates for the treatment of *S. pneumoniae* infections resistant to other antibiotics.**

Antibiotic resistance in bacterial pathogens is a serious clinical problem. This problem affects *Streptococcus pneumoniae* (the pneumococcus), which, in addition to being one of the principal human pathogens, is the main ethyological agent of community-acquired pneumonia. Annually, approximately one million children aged <5 years die of pneumococcal pneumonia, meningitis, and/or sepsis worldwide (1). Resistance to currently used antimicrobial drugs for the treatment of pneumococcal infections, including β-lactams and macrolides, has spread worldwide in the last two decades (2). The new fluoroquinolones, such as levofloxacin and moxifloxacin, which act on type II DNA topoisomerases, are therapeutic alternatives for treatment of adult patients with community-acquired pneumonia (3). However, although resistance to fluoroquinolones in *S. pneumoniae* is still lower than 3% (4), an increase in resistance is likely to occur.

DNA topoisomerases participate in almost all cellular functions involving DNA transactions (5). They solve the topological problems associated with DNA replication, transcription, and recombination. In addition, these enzymes fine-tune the steady-state level of DNA supercoiling, both facilitating protein interactions with the DNA and preventing excessive supercoiling that is deleterious. In bacteria, the homeostasis of DNA supercoiling is maintained by the opposing activities of topoisomerases that relax DNA and gyrase that introduces negative supercoils. The transcriptional response to DNA relaxation involves genes coding for all the DNA topoisomerases from *S. pneumoniae*: topoisomerase I, topoisomerase IV, and DNA gyrase. Relaxation of DNA triggers the transcriptional up-regulation of gyrase and the down-regulation of topoisomerase I and topoisomerase IV (6).

The enzymatic activity of topoisomerases involves DNA cleavage and the formation of a transient phosphodiester bond between a catalytic tyrosine residue in the protein and one of the ends of the broken strand. DNA topology is modified during the lifetime of the covalent intermediate, and the enzyme is released as the DNA is religated. Topoisomerases are classified into two types based on their DNA cleavage pattern: type I enzymes that only cleave one DNA strand and type II enzymes that cleave both strands. The type II topoisomerases are tetrameric proteins formed by two different subunits: $GyrA_2GyrB_2$ for gyrase and $ParC_2ParE_2$ for topoisomerase IV. Fluoroquinolones inhibit type II enzymes and mainly affect chromosome replication. They also stabilize a reaction intermediate in which the enzymes are covalently linked to the DNA originating double-stranded breaks that lead to cell death (7). Genetic and biochemical studies have shown that in Gram-positive bacteria, including *S. pneumoniae*, topoisomerase IV is the primary target for most fluoroquinolones, and gyrase is a secondary target (8, 9). The type I enzymes are classified as either subfamily type IA if the protein links to the 5′ phosphate or subfamily type IB when the

* The work was supported by Comunidad de Madrid Grant CM-BIO0260-2006, COMBACT (to J. H. and A. G. C.); Spanish Ministry of Science and Innovation Grants BIO2008-02154 (to A. G. C.), BFU2008-01711 (to J. A. H.), and SAF2008-03477 (to M. J. S.); and Spanish Ministry of Health, Carlos III Health Institute Grants RIER, RD08/0075/0016 (to M. J. S.).

[S] The on-line version of this article (available at http://www.jbc.org) contains supplemental Figs. S1 and S2.

[1] To whom correspondence should be addressed: Carretera a Pozuelo Km 2, 28220 Majadahonda, Madrid, Spain. Fax: 34-91-509-7919; E-mail: agcampa@isciii.es.

protein attaches to the 3′ phosphate. There is extensive sequence similarity among members of the same subfamily (10) but almost no sequence or structural similarity between the two subfamilies (11, 12). All bacterial type I topoisomerases are type IA enzymes. The overall structure of *Escherichia coli* topoisomerase I presents four domains with the active site located at the intersection of domains I and III where the catalytic Tyr-319 residue is placed (13). The proposed mechanism of action involves the opening of the enzyme through a large conformational change that separates domains II and III from the rest of the protein (14). A nucleotide-binding site has been identified in *E. coli* at the interface of domains I, III, and IV. This nucleotide-binding site, the only one formed by residues from the three domains in the closed conformation, has been proposed to bind the region of the 3′-OH end of the cleaved DNA strand (14).

Cheng *et al.* (15) have recently described one phenanthrene alkaloid able to inhibit the relaxation activity of *E. coli* topoisomerase I. However, no significant inhibition in cell growth was observed. The aim of the present study was to investigate the therapeutic potential of targeting pneumococcal topoisomerase I. For this purpose new alkaloid inhibitors of its enzymatic activity have been developed and tested for their effects on DNA supercoiling. Furthermore, their effect on cell growth was also evaluated.

EXPERIMENTAL PROCEDURES

Bacterial Strains, Growth, and Transformation of Bacteria—*S. pneumoniae* was grown in a casein hydrolysate-based medium with 0.3% sucrose as an energy source (AGCH medium) and transformed with chromosomal or plasmid DNA as described previously (16). Minimal inhibitory concentrations (MICs)[2] were determined in the same medium by the microdilution method according to the National Committee for Clinical Laboratory Standards (17). The MIC was defined as the lowest concentration of drug without visible growth.

Structures of N-Metilseconeolitsine and Seconeolitsine—The structural elucidation of compounds 16 (*N*-metilseconeolitsine) and 17 (seconeolitsine) were determined by ^{1}H and ^{13}C NMR using one-dimensional and two-dimensional (homonuclear COSY, heteronuclear multiple quantum coherence, and heteronuclear multiple bond connectivity) experiments in conjunction with mass spectral analysis and UV spectrum. The parameters were: seconeolitsine: $C_{19}H_{17}NO_4$; mp 111–113 °C; UV (MeOH): λ_{max} (log ϵ) = 262 (0.40), 289 (0.12), 325 (0.07) nm; ^{1}H-RMN (Me_2SO-d_6) δ (ppm): 2.32 (3H, *s*, N-CH_3), 2.76 (2H, *m*, $CH_{2\alpha}$), 3.14 (2H, *m*, $CH_{2\beta}$), 6.16 (2H, *s*, OCH_2O-6,7), 6.24 (2H, *s*, OCH_2O-3,4), 7.22 (1H, *s*, H-2), 7.40 (1H, *s*, H-8), 7.56 (1H, *d*, *J* = 9.3 Hz, H-9), 7.81 (1H, *d*, *J* = 9.3 Hz, H-10), 8.39 (1H, *s*, H-5); ^{13}C-RMN (Me_2SO-d_6) δ (ppm): 32.88 ($CH_{2\beta}$), 35.75 (NCH_3), 52.73 ($CH_{2\alpha}$), 100.93 (OCH_2O, C-3,4), 101.48 (OCH_2O, C-6,7), 104.37 (C-5), 105.19 (C-8), 110.29 (C-2), 116.28 (C-4a), 121.31 (C-10), 123.44 (C-5a), 124.32 (C-9), 125.01 (C-10a), 128.15 (C-8a), 131.33 (C-1), 140.64 (C-4), 144.03 (C-3), 147.03* (C-7) 147.10* (C-6); EI-MS *m/z* (relative intensity) = 323 (10), 280 (100), 279 (32), 221 (2), 163 (14); and *N*-Metilseconeolitsine: $C_{20}H_{19}NO_4$; mp 132–134 °C; UV (MeOH): λ_{max} (log ϵ) = 262 (0.40), 289 (0.12), 325 (0.07) nm; ^{1}H-RMN (Me_2SO-d_6) δ (ppm): 2.22 (6H, *s*, N-$(CH_3)_2$), 2.49 (2H, *m*, $CH_{2\alpha}$), 3.12 (2H, *m*, $CH_{2\beta}$), 6.17 (2H, *s*, OCH_2O-6,7), 6.25 (2H, *s*, OCH_2O-3,4), 7.25 (1H, *s*, H-2), 7.41 (1H, *s*, H-8), 7.57 (1H, *d*, *J* = 9.3 Hz, H-9), 7.75 (1H, *d*, *J* = 9.3 Hz, H-10), 8.39 (1H, *s*, H-5); ^{13}C-RMN (Me_2SO-d_6) δ (ppm): 30.79 ($CH_{2\beta}$), 45.10 ($N(CH_3)_2$), 60.51 ($CH_{2\alpha}$), 100.94 (OCH_2O, C-3,4), 101.48 (OCH_2O, C-6,7), 104.39 (C-5), 105.19 (C-8), 110.29 (C-2), 116.28 (C-4a), 121.15 (C-10), 123.47 (C-5a), 124.40 (C-9), 124.90 (C-10a), 128.12 (C-8a), 131.50 (C-1), 140.60 (C-4), 144.05 (C-3), 146.80 (C-6) 146.80 (C-7); EI-MS *m*/*z* (int. rel.) = 337 (100), 279 (63), 221 (5), 191 (5), 163 (58).

Cloning and Expression of topA in E. coli—The *topA* gene was amplified by PCR with 0.1 μg of chromosomal DNA from *S. pneumoniae* R6 and 1 μM (each) synthetic oligonucleotide primers. The oligonucleotides used were topAUP2 (5′-GTG-GCTACGGCAACAAAAAAGAA-3′) and topADOWN (5′-cgcgcgcatgcTTATTTAATCTTTTCTTCCTC-3′). The 5′ end of topADOWN contained a sequence including a PaeI restriction site (lowercase letters), topAUP2 included the GTG initiation codon, and topADOWN included the sequence complementary to the TAA stop codon (underlined). Amplification was achieved with an initial cycle of 2 min of denaturation at 94 °C, 1 min of annealing at 55 °C, and 2.5 min of polymerase extension with *Pfu* high fidelity polymerase (Fermentas) at 72 °C and then 30 cycles of 2 min at 94 °C, 1 min at 55 °C, and 2.5 min at 72 °C with slow cooling at 10 °C. The oligonucleotides were removed (QIAquick PCR purification kit; Qiagen), cut with PaeI, cloned into plasmid pQE1 digested with PaeI and PvuII, and established in *E. coli* M15 (pREP4) (Qiagen). Sequencing with oligonucleotides pQE-seq3 (5′-AGCTAGC-TTGGATTCTCACC-3′) and pQE-seq5 (5′-GAGGCCCTTT-CGTCTTCA-3′) was performed to confirm the cloning. The pQE1 vector/M15(pREP4) host cloning system permits the hyperproduction of His_6-tagged recombinant proteins encoded by genes placed under the control of a phage T5 promoter and two *lac* operator sequences. The host strain contains the low copy plasmid pREP4, which constitutively expresses the LacI repressor. Expression of recombinant proteins encoded by pQE vectors was induced by the addition of isopropyl-β-D-thiogalactoside (IPTG), which binds to the LacI protein and inactivates it. This inactivation allows the RNA polymerase of the host cell to transcribe the sequences downstream from the T5 promoter. A culture of *E. coli* M15 (pREP4)/pQE-SPNtopA was grown at 37 °C in LB medium containing 250 μg/ml of ampicilin (to select pQE1) and 25 μg/ml kanamycin (to select pREP4) to A_{620} = 0.6. IPTG (1 mM) was added, and incubation was continued for 30 min. The cells were collected by centrifugation, lysed at 4 °C for 30 min in buffer A (50 mM NaH_2PO_4, pH 8, 300 mM NaCl, 10 mM imidazol) and lisozyme (1 mg/ml), and sonicated for 5 min (10 times for 30 s, with 1 min cooling between each sonication) in a Sonifier B-12 (Branson Co.). Debris was removed

[2] The abbreviations used are: MIC, minimal inhibitory concentration; IPTG, isopropyl-β-D-thiogalactoside; PI, propidium iodide; GA, genetic algorithm; CCC, covalently closed negatively supercoiled; TOPO1, topoisomerase I.

by centrifugation at 10,000 × *g* for 20 min, and the resulting supernatant was dialyzed overnight against buffer A. The TopA protein was purified by affinity chromatography in a nickel-nitrilotriacetic acid (Qiagen) column following manufacturer's instructions. Briefly, the column (1 ml) was washed with 10 ml of buffer A, and the bound proteins were eluted with 10 ml of buffer containing imidazol at 60, 100, and 200 mM. Fractions of 2 ml were collected and analyzed by SDS-10% polyacrylamide gel and stained with Coomassie Blue. Fractions containing a protein of the expected size were dialyzed against buffer B (20 mM Tris-HCl, pH 8, 50 mM KCl, 1 mM DTT, 50% glycerol). The purified protein was conserved at −20 °C. In these conditions, TopA remains active for at least 12 months.

Cloning of topA under the Control of Pmal in S. pneumoniae—The *topA* gene was amplified by PCR from strain R6 as described above except that primer topAUP4 (5′-cgcgctctagaAGGTGTGATACTATGGCT-3′) was used instead of topAUP2. The 5′ end of topAUP4 contained a sequence including an XbaI restriction site (lowercase letters) and included an ATG initiation codon (underlined). The amplified fragment was cut with PaeI + XbaI, cloned into plasmid pLS1RGFP (18) digested with the same enzymes, and established in strain R6. Transformed bacteria were selected in AGCH containing erythromycin (1 μg/ml). Recombinant plasmids were identified by digestion with HindIII + EcoRI and confirmed by sequencing with oligonucleotides pLS1rF (5′-GAGTATACTTATAAGTAACGCAAAC-3′) and pLS1rR (5′-TAGGTTGAGGCCGTTGAGCACC-3′).

Relaxation of pBR322 by TopA and Human TOPO1—Reactions were carried out in 15 or 100 μl containing 0.5 μg of supercoiled plasmid pBR322 in 20 mM Tris-HCl, pH 8, 100 mM KCl, 10 mM $MgCl_2$, 1 mM DTT, 50 μg of BSA/ml. After 1 h of incubation at 37 °C in the presence on TopA, the reaction was terminated by 2 min of incubation at 37 °C with 50 mM EDTA and 1 h at 37 °C with 1% SDS, 100 μg/ml proteinase K. Treatment with human TOPO1 (Inspiralis, Norwich, UK) was performed with the buffer and conditions recommended by the supplier. When required, the samples were ethanol-precipitated and resuspended in H_2O. The reaction products were analyzed by electrophoresis in 1.2% agarose gels run at 18 V for 20 h. Treatment with the alkaloids was performed by preincubation of TopA or TOPO1 for 10 min at 4 °C in a final volume of 15 μl. DNA quantification of agarose gels was done by scanning densitometry after electrophoresis and EtBr staining. Quantification of TopA activity was calculated by gel densitometry using the Quantity One program (Bio-Rad). To calculate activity, the amount of the covalently closed negatively supercoiled (CCC) form was determined and divided by the total amount of DNA in each well. IC_{50} (mean of at least three independent determinations) was defined as the concentration of drug required for a 50% reduction of enzymatic activity.

Analysis of the Topology of Covalently Closed Circles—Circular DNA molecules were analyzed in neutral/neutral two-dimensional agarose gels. The first dimension was run at 1.5 V/cm in a 0.4% agarose (Seakem; FMC Bioproducts) gel in 1× Tris borate-EDTA (TBE) buffer for 17–19 h at room temperature. The second dimension was run at 7.5 V/cm in 1% agarose gel in 1× TBE buffer for 7–9 h at 4 °C. Chloroquine (Sigma) was added to the TBE buffer in both the agarose and the running buffer. After electrophoresis gels were subjected to Southern hybridization. Two probes were used on two-dimensional agarose gels transferred to nylon membrane (Inmobylon NY^+; Millipore). For the analysis of the supercoiling level in pLS1 *in vivo*, a 240-bp PCR fragment obtained from pLS1 as described (6) was used. For the analysis of the enzymatic activity of TopA, pBR322 plasmid was digested with EcoRI + EcoRV, and the ends were filled with biotinylated dNTPs by the Klenow polymerase fragment (Fermentas) and used as a probe. Chemiluminiscent detection of DNA was performed with the Phototope®-Star kit (New England Biolabs). Images were captured in a VersaDoc MP400 system and analyzed with the Quantity One program (Bio-Rad).

Cytofluorometric Analysis of Neutrophil Apoptosis and Survival—Human peripheral blood neutrophils were obtained from buffy coats of healthy donors by Ficoll Hypaque density gradient centrifugation, as described previously (19). Freshly isolated neutrophils were resuspended in supplemented RPMI medium at 2×10^6 cells/ml. Twenty-five μl were cultured in a 96-well plate containing 200 μl of supplemented RPMI medium for 24 h in the absence or presence of compounds 16 and 17. Assessment of apoptosis was performed by flow cytometry using annexin V-FITC and propidium iodide (PI). The protocol indicated by the manufacturer (Annexin-V-Fluos; Roche Applied Science) was used as outlined previously (20). Cells (1×10^4) were analyzed in a Beckman Coulter Epics XL (Fullerton, CA) and differentiated as early or viable apoptotic (annexin V^+ and PI^-), late apoptotic and/or necrotic (annexin V^+ and PI^+), and viable nonapoptotic (annexin V^- and PI^-) cells.

EtBr Displacement Assay—A total of 6 μg (300 μl) of calf thymus DNA was diluted to 3 ml with buffer (20 mM NaCl, 2 mM HEPES, 10 μM EDTA, pH 7.4). Prior to analysis, 3 μl of EtBr (0.5 mg/ml) were added and allowed to equilibrate for 1 min. Aliquots of alkaloids were then added, and the fluorescence was measured on an Cary Eclipse Varian fluoresce spectrophotometer after 1 min of equilibration, using excitation and emission wavelengths of 546 and 660 nm, respectively.

Molecular Modeling of Topoisomerase I from S. pneumoniae—The model was built on the basis of the crystal structure of *E. coli* topoisomerase I (Protein Data Bank code 1CY1). Amino acid changes along the entire sequence were performed using the O program (21), running in a Silicon Graphics work station. Side chain rotamers were chosen from a database of more common conformers. The overall fold of the model was energy-minimized using the minimizer algorithm implemented in the CNS package (22). The stereo chemical quality of the model was checked with the PROCHECK program (23).

Three-dimensional Structures of Alkaloid Ligands and Molecular Docking—Boldine, secoboldine, seconeolitsine, and *N*-methyl-seconeolitsine were used in the docking calculations. The three-dimensional structures of boldine and secoboldine were obtained from the Cambridge Structural

Database with reference codes HIHXUR and OLIDES, respectively. The three-dimensional structures of seconeolitsine and *N*-methyl-seconeolitsine were modeled on the basis of the crystallographic structures of boldine and secoboldine by using the Dundee PRODRG2 Server (24). Stereochemistry of ligands was checked with the Mercury program (25). Molecular docking was carried out using GOLD (Genetic Optimization for Ligand Docking) software (26), which uses the genetic algorithm (GA). This method allows a partial flexibility of protein and full flexibility of the ligand. The cavity was defined from to 10 Å around Ser-487, giving freedom of movement to Asp-101, Arg-102, Arg-156, Arg-300, Arg-485, Asp-543, and Glu-546 in side chain rotamers. For each of the 25 independent GA runs, a maximum number of 100,000 GA operations were performed on a set of five groups with a population size of 100 individuals. Default cut-off values of 2.5 Å (dH-X) for hydrogen bonds and 4.0 Å for van der Waals distance were employed. When the top three solutions attained RMSD values within 1.5 Å, GA docking was terminated. The RMSD values for the docking calculations are based on the RMSD matrix of the ranked solutions. We observed that the best ranked solutions were always among the first 10 GA runs, and the conformation of molecules based on the best fitness score was further analyzed.

RESULTS

Characterization of the DNA Topoisomerase I of S. pneumoniae—We performed a BLAST search for DNA topoisomerases coding sequences in the *S. pneumoniae* R6 genome (27) and found that, in addition to the genes coding the two type II enzymes (gyrase and topoisomerase IV), gene *topA* (spr1141) encodes an homologue of bacterial topoisomerase I. The topoisomerase I enzymes from *E. coli* and *S. pneumoniae* show 46.9% similarity on the whole sequence and 62% in the cleavage/strand passage module (Fig. 1*A*). The *topA* gene was amplified by PCR from R6 chromosomal DNA with specific oligonucleotides and cloned into the *E. coli* plasmid pQE-1 rendering pQE-SPNtopA, which carries the Met-His_6-Gln-TopA fusion protein under the control of the T5 promoter. This plasmid was established into *E. coli* M15 (pREP4), and its T5 promoter was induced by IPTG. The recombinant plasmid overproduced a protein with apparent molecular mass of 84 kDa and an apparent purity of 98% (Fig. 1*B*), which is in agreement with the expected size of the fusion protein (79.37 kDa for TopA + 5.23 kDa for the N-terminal fusion). The total yield of purification was 0.8 mg of purified TopA per liter of culture, with a concentration of 80 μg/ml and a specific relaxation activity (see below) of 2.4×10^4 units/mg.

To test DNA relaxation activity of TopA, the CCC pBR322 plasmid (1.77 nM) was incubated in the presence of different amounts of the purified enzyme, and the reaction products were analyzed in mono-dimensional agarose as described (28, 29). TopA activity converted the CCC plasmid in topoisomers with different degrees of supercoiling that were observed as discrete bands when the gel was run in the absence of EtBr (Fig. 2*A*). However, all of the relaxed topoisomers migrated as a single band when the gel was run in the presence of saturating concentrations of EtBr (Fig. 2*B*). A unit of TopA enzymatic activity was defined as the amount of enzyme being able to relax 50% of the CCC substrate in 1 h at 37 °C and corresponded to 42 ng (5 nM) of the purified enzyme. As observed in other bacterial topoisomerase I enzymes, the pneumococcal TopA did not relax positively supercoiled DNA (Fig. 2*C*). This was shown by the absence of activity on CCC pBR322 treated with EtBr (Fig. 2*C*, *lane +EtBr*), which, at the high concentration used, introduces positive supercoiling. The activity was partially recovered when the intercalating agent was removed with isoamyl alcohol (Fig. 2*C*, *lane ±EtBr*). An additional method to examine pBR322 topoisomer distribution after TopA treatment was two-dimensional agarose gel electrophoresis in the presence of chloroquine (30). This technique, which differs from the classical two-dimensional chloroquine gels, makes it possible to separate DNA molecules by mass and shape. In the two-dimensional gel, topoisomers appeared distributed in the autoradiograms in a bubble-shaped arc, negative supercoiled molecules were located on the right side, and positive supercoiled ones were located on the left (Fig. 2, *D* and *E*). In the absence of enzyme, 100% of the topoisomers had negative supercoiling (Fig. 2*D*). In the presence of 1 unit (5 mM) of enzyme, 56.8 and 43.2% were negative and positive supercoiled topoisomers, respectively. In the presence of 3 units (15 mM) of TopA, these figures were 16.8 and 83.2% for negative and positive supercoiled topoisomers, respectively (Fig. 2*D*).

Inhibition of TopA Activity by Aporphine and Phenanthrene Alkaloids—A total of 18 compounds (six aporphine and 12 phenanthrene alkaloids; supplemental Fig. S1) semisynthesized from the natural alkaloid boldine (Ref. 31 and data not shown) were selected to test inhibition of growth and inhibition of *S. pneumoniae* TopA activity. As shown in Table 1, previously characterized clinical isolates (4), either susceptible or resistant to various antibiotics (including fluoroquinolone resistant), were tested. The alkaloids showed equivalent activities against all isolates, independently of their antibiotic resistance, suggesting the absence of cross-resistance. Two phenanthrene alkaloids, with numbered compounds 16 and 17 (Fig. 3), showed the greatest inhibition of growth. The structural elucidation of these compounds was carried out as described under "Experimental Procedures."

The *in vitro* inhibition of TopA relaxation activity was tested with the 18 compounds using 1 unit of enzyme, *i.e.* the amount of enzyme yielding 50% of activity. Under these conditions, TopA relaxation activity was inhibited in a concentration-dependent manner, with IC_{50} values (average ± S.D.) of 559 ± 72.0 ($n = 3$) for secoboldine (compound 2), 58.2 ± 3.0 ($n = 3$) for neolitsine (compound 14), 17 ± 0.4 ($n = 5$) for *N*-methyl-seconeolitsine (compound 16), and 17 ± 0.4 μM ($n = 4$) for seconeolitsine (compound 17) (Fig. 4, *A* and *B*). A good correlation ($r^2 = 0.96$) between the inhibition of TopA activity and the inhibition of cell growth was observed for these compounds. These results imply that topoisomerase I is indeed the *in vivo* target of the compounds assayed. The inhibition by the alkaloids was enhanced by preincubation of the enzyme with the drug. Lower inhibition was observed when preincubation was avoided (Fig. 4*C*). These results suggest

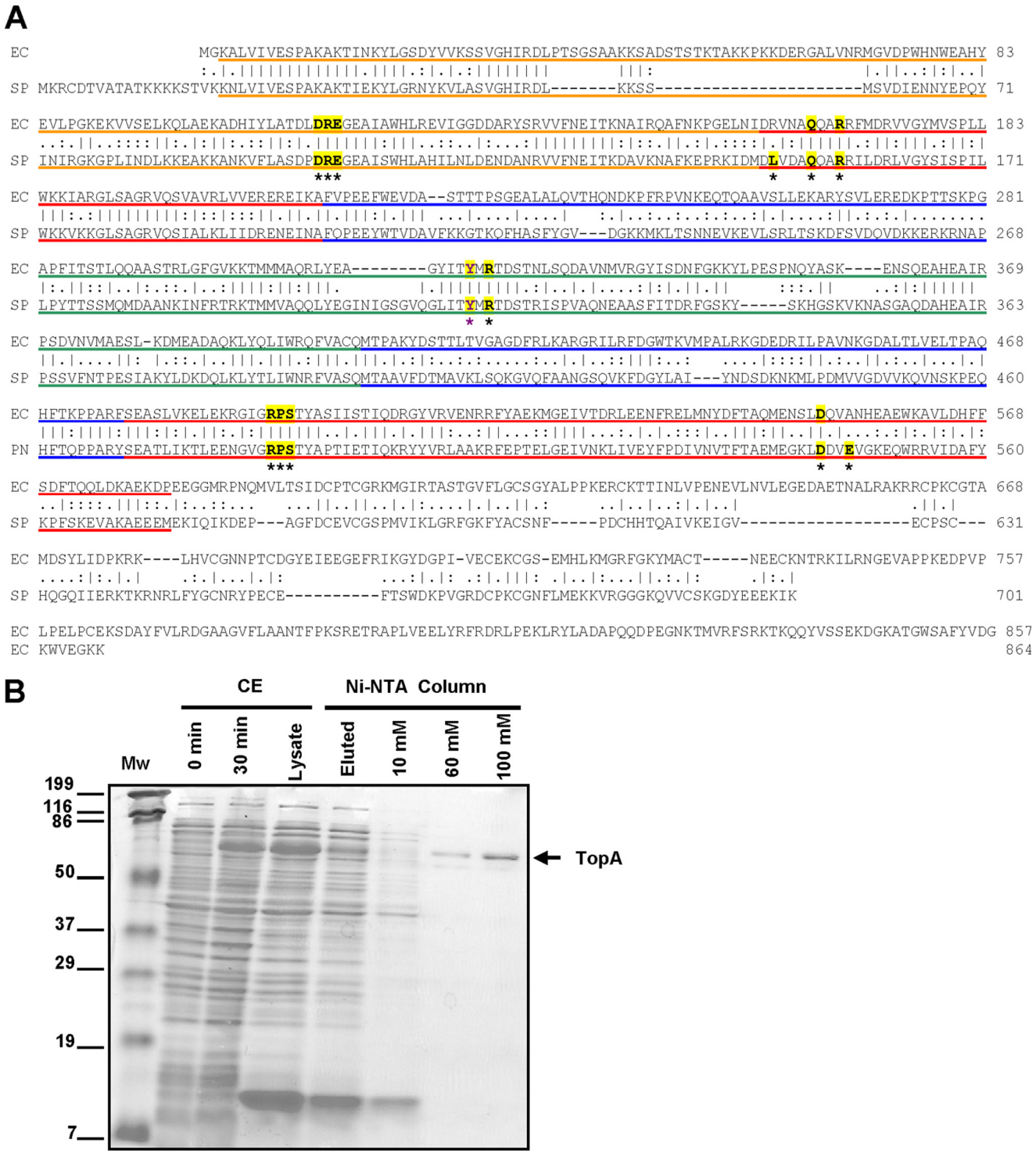

FIGURE 1. **Identification and purification of *S. pneumoniae* DNA topoisomerase I.** *A*, alignment of *E. coli* and *S. pneumoniae* TopA proteins. Color codes correspond to the four structural domains showed in Fig. 7. The catalytic Tyr residue (Tyr-319 for *E. coli* and Tyr-314 for *S. pneumoniae*) is *magenta*, highlighted in *yellow*, and labeled with a *magenta asterisk*. Residues in *bold type* labeled with a *black asterisk* and highlighted in *yellow* form part of the nucleotide-binding site and are involved in the salt bridge interaction network. *B*, expression of TopA and steps of purification. Cultures of M15 (pREP4) containing pQE-SPNtopA were grown in LB medium and induced with IPTG as described under "Experimental Procedures." Samples of 10 μl were electrophoresed in a SDS-10% polyacrylamide gel. The polypeptides were revealed by Coomassie Blue staining. *CE*, crude extract *lanes*, 12 μg after 0 and 30 min induction; *Ni-NTA column lanes*, fraction that did not bind to the column and eluted in the loading (9 μg), fraction eluted with 10 mM (2 μg), with 60 mM (0.5 μg) and 100 mM (1 μg) imidazol. The sizes of protein markers (*Mw*) are indicated to the *left*.

that the alkaloid would interact with the enzyme at the DNA-binding site (see below).

Some inhibition of the relaxation activity over pBR322 was observed for compounds 2 and 5 at concentrations $\geq$100 μM (Fig. 4*A*). However, no inhibition for boldine (Fig. 4*A*) and the rest of the compounds (data not shown) was observed at concentrations $\leq$500 μM. The inhibition of TopA was tested with EtBr, a typical DNA intercalant compound. A pattern com-

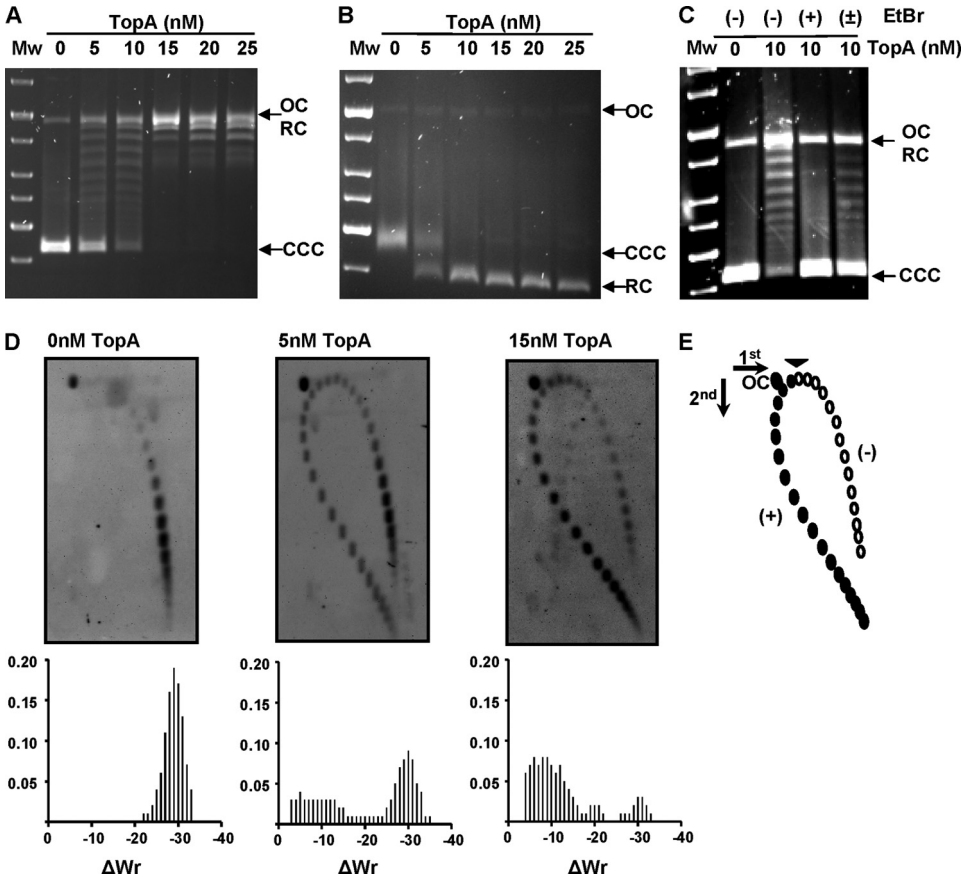

FIGURE 2. **TopA has nicking and closing activities.** Plasmid pBR322 (1.77 nM) was incubated with purified topoisomerase I at the indicated concentrations for 1 h at 37 °C. The samples were processed and analyzed as described under "Experimental Procedures." *OC*, relaxed open circles; *CCC*, covalently closed circles; *RC*, relaxed circular plasmids forms. *Mw*, molecular mass standard. *A*, gel run in the absence of EtBr. *B*, the same samples run in *A* were run in the presence of 0.5 μg/ml of EtBr. *C*, TopA activity on positively supercoiled pBR322. In wells labeled as (+) for EtBr, the pBR322 was incubated in the presence of 2 μg/ml of EtBr for 15 min at 4 °C before the incubation with TopA. In the well labeled (±), pBR322 previously treated with 2 μg/ml of EtBr was treated with isoamylalcohol to remove EtBr and further incubated with TopA. *D*, topoisomer distribution of pBR322 after TopA treatment. Plasmid DNA was subjected to two-dimensional agarose electrophoresis. *E*, illustration of pBR322 topoisomer distribution after treatment with 15 mM TopA in two-dimensional electrophoresis in agarose gels run in the presence of 1 and 2 μg/ml chloroquine in the first and second dimensions, respectively. Negative supercoiled topoisomers are in *white*, and positive supercoiled are in *black*. A *black arrowhead* indicates the topoisomer that migrated with $\Delta Lk = 0$ in the second dimension.

TABLE 1
Susceptibilities of *S. pneumoniae* strains to boldine derivatives

Strains	Resistance pattern[a]	MIC[b]												
		2	3	4	5	6	7	11	12	13	14	16	17	23
		μM												
R6	S	500	500	>250	500	250	250	125	125	500	125	16	16	62
ATCC 6303	S	1000	1000	>250	500	>250	250	125	125	500	125	16	16	125
CipS8	S	500	500	>250	500	>250	125	125	125	500	125	16	16	62
CipS9	S	1000	1000	>250	1000	>250	250	125	125	500	125	16	16	125
CipR20	PTCEClSxTCip	1000	500	>250	250	>250	250	125	125	500	62	8	16	125
CipR16	PSxTCip	1000	1000	>250	500	>250	500	125	125	500	125	16	16	62
CipR8	PSxTCip	500	500	>250	500	>250	250	62	125	500	62	8	8	125
CipR42	PTEClCip	1000	1000	>250	500	>250	250	125	125	500	62	8	8	125
CipR45	TEClCip	500	500	>250	1000	>250	250	125	125	500	62	8	16	125
CipR68	Cip	500	500	>250	500	>250	250	125	125	500	62	8	8	125
CipR5	EClCip	500	500	>250	500	>250	250	125	125	500	62	16	16	62
CipR15	SxTCip	1000	1000	>250	500	>250	250	125	125	500	62	16	8	62

[a] S, susceptible to all antibiotics tested; P, resistant to penicillin (MICs of 0.12–4 μg/ml); T, resistant to tetracycline (MICs ≥4 μg/ml); C, resistant to chloramphenicol (MIC ≥ 8 μg/ml); E, resistant to erythromycin (MIC ≥ 0.5 μg/ml); Cl, resistant to clindamycine (MIC ≥ 1 μg/ml); Cip, resistant to ciprofloxacin (MIC ≥ 4 μg/ml), SxT, resistant to cotrimoxazole (MIC ≥ 4 μg/ml for trimethoprim and MIC ≥ 76 μg/ml for sulfamethoxazole).
[b] MICs for compounds B (boldine), 10, 19, 20, 21, and 22 were 1000 μM in all cases. The chemical structures of the compounds used are showed in supplemental Fig. S1.

patible with the intercalation of EtBr into the CCC pBR322 form was observed (Fig. 4*C*). In addition, preincubation did not change the observed pattern. These results suggest that TopA was not inhibited by EtBr.

Human topoisomerase I, a prototype IB topoisomerase, was tested in relaxation assays with compounds 16 (*N*-metilseconeolitsine) and 17 (seconeolitsine) (Fig. 5*A*). Activation was observed at low concentrations and partial inhibition at 50

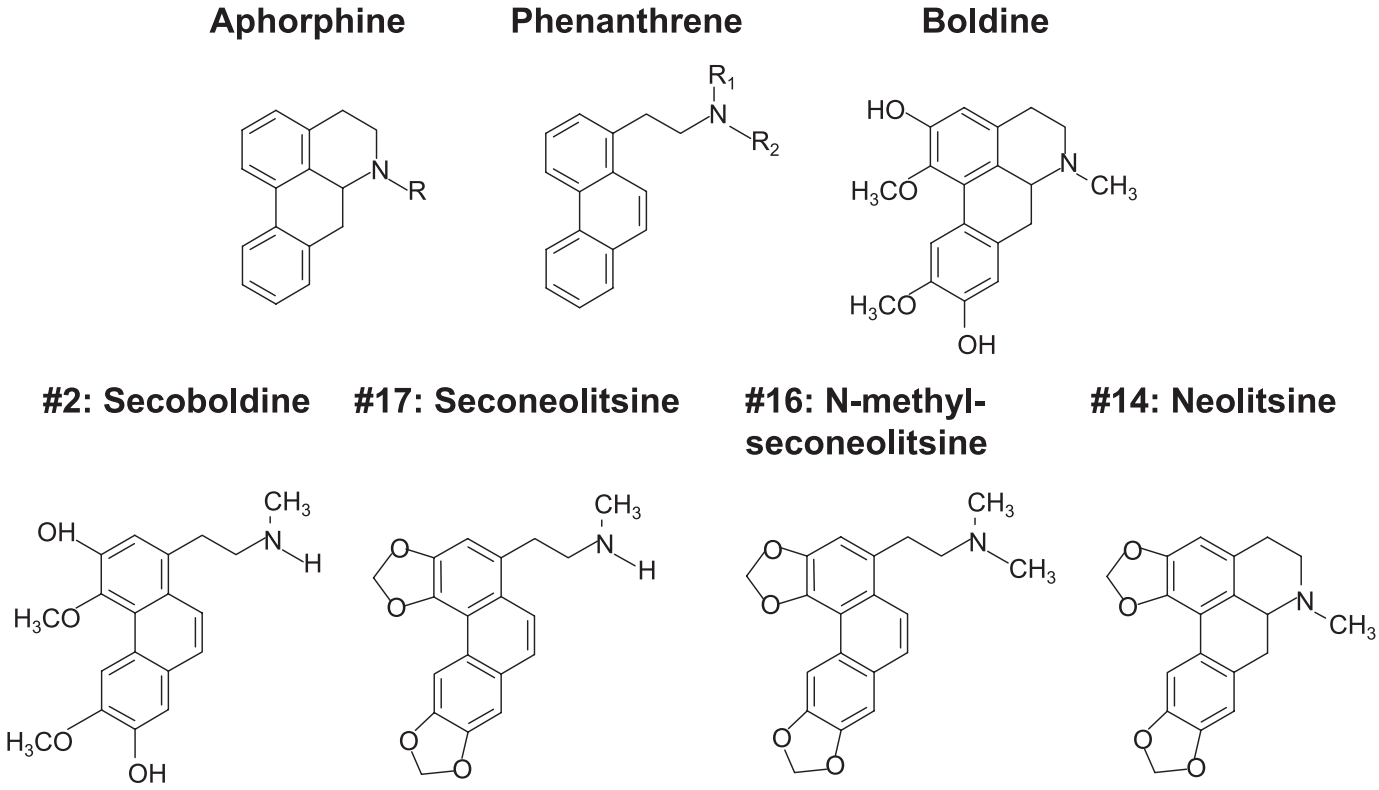

FIGURE 3. **Chemical structures of the most relevant aporfine and phenantrene alkaloids used in this study.**

μM, a concentration at which the pneumococcal TopA showed full inhibition (data not shown). These effects on topoisomerase I could be attributed to the intercalation of compounds 16 and 17 in the DNA. As showed in Fig. 5*B*, both compounds displace EtBr from calf thymus DNA. At 50% displacement, the ratio alkaloid/EtBr was 2.5 (compound 16) and 2.8 (compound 17).

Targeting of TopA in Vivo by Seconeolitsine—To assess whether TopA is the *in vivo* target of the alkaloids, different attempts were made to obtain mutants resistant to these compounds. Approximately 1.2×10^{10} cells were plated on agar plates containing 1 to 8 × MIC (minimal inhibitory concentration) of seconeolitsine, and no resistant bacteria were obtained. Therefore, to establish that the primary cellular target for the phenanthrene alkaloids was indeed topoisomerase I, the *topA* gene was cloned under the control of the Pmal promoter into plasmid pLS1R, yielding plasmid pLS1R-topA. The activity of this promoter was induced by maltose (18). The effect of the drug was tested in the wild type strain R6 (seconeolitsine MIC = 16 μg/ml) carrying either pLS1R or pLS1R-topA plasmids, at drug concentrations ranging from 0.25× to 1× MIC. These results show that cell growth (Fig. 6*A*) and division (Fig. 6*B*) were affected in a drug concentration-dependent manner. The growth of R6 carrying either of these plasmids showed similar kinetics in the absence or presence of seconeolitsine at 1× MIC the drug (Fig. 6). In contrast, differences in both growth inhibition and viability were observed at 0.25 × MIC and 0.5 × MIC, where inhibition by seconeolitsine was attenuated by the induction of TopA in plasmid pLS1R-topA (Fig. 6).

Further evidence of the *in vivo* inhibition of TopA by seconeolitsine was obtained from the analysis of topoisomers distribution of the internal plasmid pLS1 by two-dimensional agarose gel electrophoresis, a suitable approach for studying supercoiling levels (6). This technique allows separation of DNA molecules by mass and shape. First, the pLS1 linking number (ΔLk) was quantified using two-dimensional agarose gel electrophoresis with 15 μg/ml chloroquine in the second dimension. Under these conditions, the induced ΔLk of monomers was −31. Treatment with compound 16 at 0.5× MIC and 1× MIC resulted in a time-dependent increase of plasmid supercoiling (Fig. 7). At 0.5× MIC, supercoiling densities (σ) were −0.059, −0.086, and −0.093 at 0, 5, and 30 min after drug addition, respectively, indicating that plasmids became hypernegatively supercoiled. Similar results were obtained after treatment at 1 × MIC, where supercoiling densities were −0.093 and −0.100 at 5 and 30 min, respectively. Although direct extrapolation from the observations made in small plasmids is not completely equivalent to the bacterial chromosome, our results indicate that supercoiling significantly increases in the presence of seconeolitsine and support that TopA is its *in vivo* target.

Modeling of S. pneumoniae TopA and Docking with Alkaloids—We have observed a 46.9% sequence similarity between topoisomerase I enzymes from *E. coli* and *S. pneumoniae* (Fig. 1*A*). Therefore, a structural model of the pneumococcal TopA was performed based on the structure of the *E. coli* enzyme. The model shows that residues forming the active site are mainly conserved between *E. coli* and *S. pneumoniae*. The catalytic Tyr-319 of *E. coli* corresponds

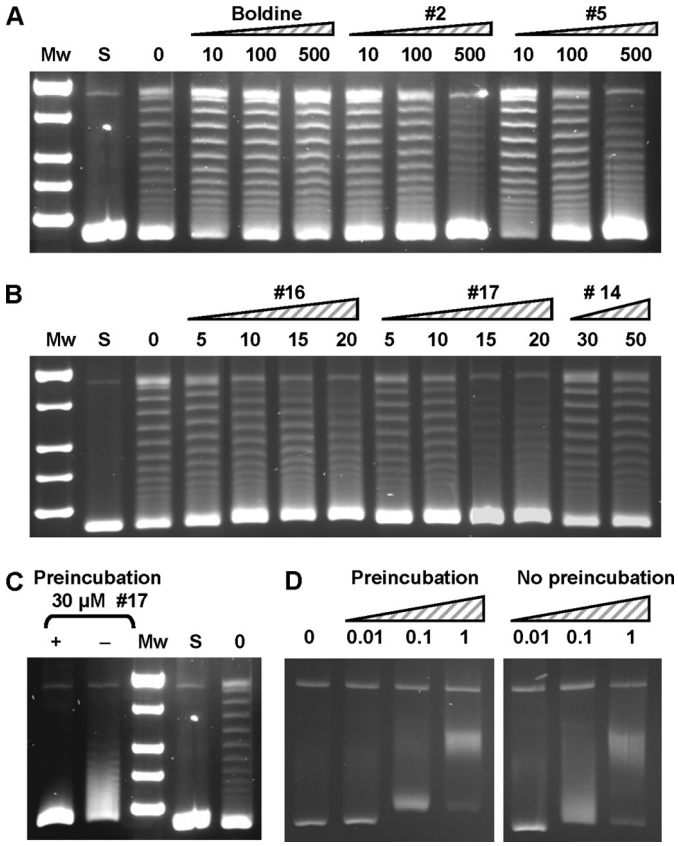

FIGURE 4. **TopA is inhibited by phenanthrene alkaloids.** *A*, inhibition of TopA by boldine, compound 2 (secoboldine) and compound 5 (*N*-methyl-secoboldine). Supercoiled pBR322 (0.5 μg) was treated with 1 unit of purified TopA in 15-μl reactions containing the alkaloids at the concentrations (μM) indicated. *Mw*, molecular mass standard; *S*, covalently closed supercoiled pBR322 used as substrate. *B*, inhibition of TopA by compounds 16 (*N*-metilseconeolitsine), 17 (seconeolitsine), and 14 (neolitsine). The reactions were carried out as in *A*. *C*, the inhibition of TopA by seconeolitsine is enhanced by preincubation of the enzyme with the alkaloid. pBR322 was treated with 1 unit of purified TopA in the absence of the inhibitor (*lane 0*), or in the presence of 30 μM of compound 17 with (*lane* +) or without (*lane* −) preincubation during 10 min at 4 °C. *D*, effect of EtBr on TopA activity. The reactions were carried out as in *A* containing the compound at the indicated concentrations (μM).

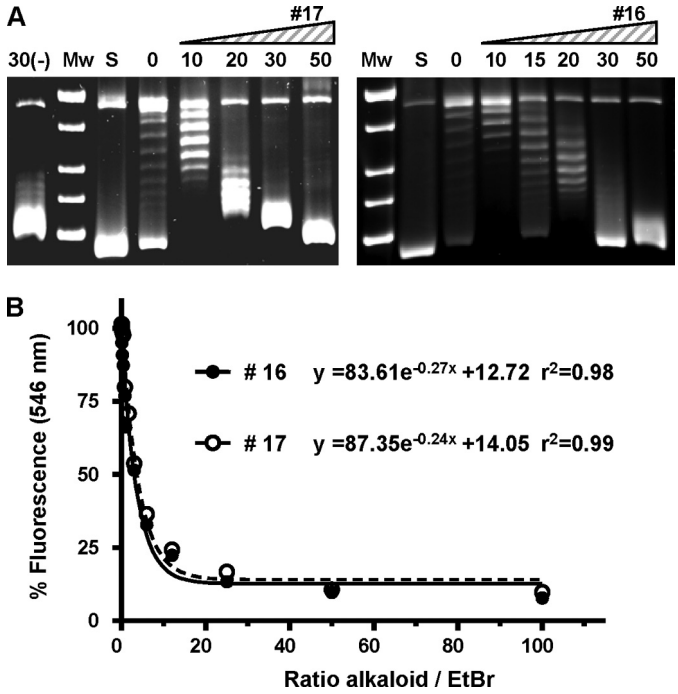

FIGURE 5. **Human TOPO1 is not inhibited by phenantrene alkaloids.** *A*, effect of compounds 16 (*N*-methyl-seconeolitsine) and 17 (seconeolitsine) on the enzymatic activity. Supercoiled pBR322 was treated with 1 unit of enzyme in the absence (*lanes 0*) or in the presence of various concentrations of the alkaloids with or without (*lane 30(-)*) preincubation 30 μM of compound 17. *B*, EtBr displacement assay of compounds 16 and 17. Fluorescence is expressed as the percentage of the maximum fluorescence signal when EtBr was bound to the DNA in the absence of the alkaloids and was corrected for background fluorescence of EtBr in solution.

to Tyr-314 of *S. pneumoniae* (Fig. 8*A*). The nucleotide-binding site (binding of the 3′-OH end of the cleaved DNA strand) has been identified in *E. coli* at the interface of domains I, III, and IV (14). The equivalent site in *S. pneumoniae* TopA presents a strong salt bridge interaction network at both sides of the cavity. This network is formed by residues Arg-485, Asp-543, Arg-102, and Glu-546 on one side and Glu-103, Arg-316, and Asp-101 on the other side (Fig. 7*C*). All of these residues are also found in *E. coli* and *Staphylococcus aureus* except for Asp-546, which is an Ala residue in *E. coli* and *S. aureus.*

Furthermore, drug recognition by the pneumococcal TopA enzyme was modeled by docking using the GOLD program with boldine, secoboldine, seconeolitsine, and *N*-methyl-seconeolitsine (Fig. 3 and supplemental Fig. S2). All of these ligands are placed in a similar orientation, stacked between Pro-486 and Arg-102 in the nucleotide-binding site (supplemental Fig. S2), as observed for the *E. coli* topoisomerase I in complex with nucleotide (13). Among all of the tested ligands, *N*-methyl-seconeolitsine displays more interactions with the protein than the remaining alkaloids (Fig. 8*C* and supplemental Fig. S2). The larger number of interactions for phenanthrene alkaloids (secoboldine, seconeolitsine, *N*-methyl-seconeolitsine) compared with those with aporphine skeleton (boldine), can be explained by the presence of a third benzylic ring. This extra ring may further stabilize the structures through both cation-π interaction with Arg-102 and a stacking interaction with Pro-486. Interestingly, Arg-102, which is critical for the cation-π interaction with the ligand, is also stabilized by a double salt bridge interaction with Asp-543 and Glu-546 (the last one unique to *S. pneumoniae).* Moreover, oxygen atoms from methylenedioxy groups are establishing polar contacts with Glu-103, Arg-156, and Asp-543. Furthermore, additional polar interaction can be predicted between the secondary amine group of *N*-methyl-seconeolitsine and Glu-546. Taking into account all of these data, the large salt bridge network in *S. pneumoniae* TopA results in a rigid and narrow cavity in which *N*-methyl-seconeolitsine is strongly stabilized through both the interactions with different protein residues and by a perfect fitting in the cavity (Fig. 8*B*).

Effect of Seconeolitsine and N-Methyl-seconeolitsine in Human Cell Viability—At the two concentrations assayed (30 and 100 μM), neither *N*-methyl-seconeolitsine nor seconeolitsine affected neutrophil apoptosis (Fig. 9). In contrast, seconeolitsine, at the highest concentration tested (100 μM), caused a small but significant decrease in neutrophil survival

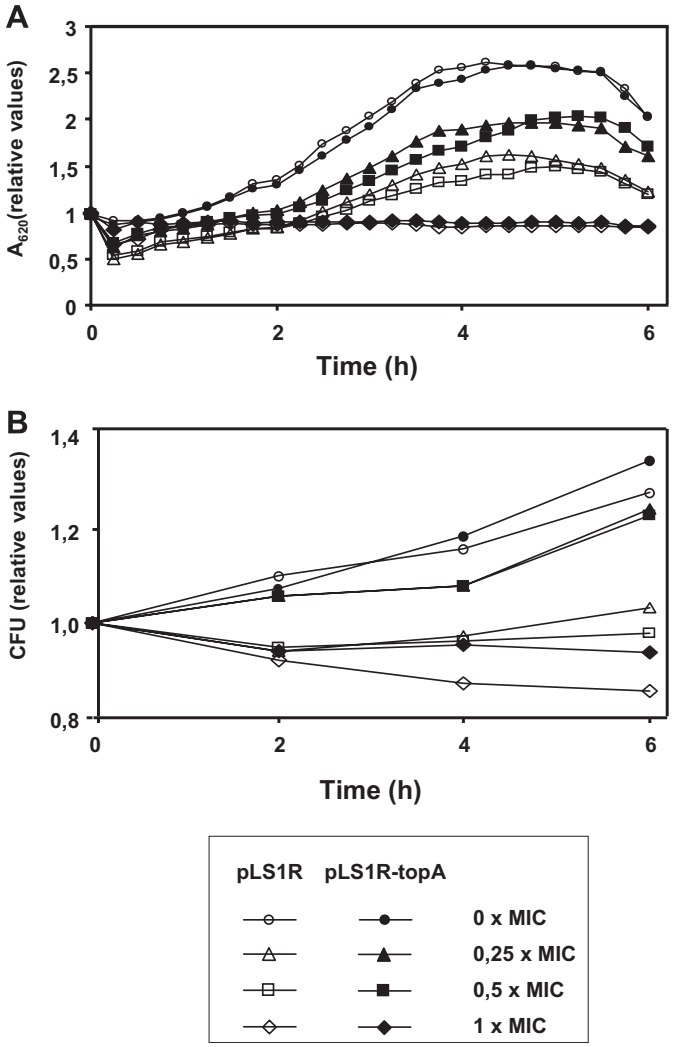

FIGURE 6. **The overexpression of TopA allows cell survival in the presence of seconeolitsine.** Exponentially growing cultures of R6 carrying pLS1R (*open symbols*) or pLS1R-topA (*full symbols*) were grown in AGCH containing 0.8% sucrose to $A_{620} = 0.6$. At this moment, the cultures were diluted 20-fold in medium containing 0.4% sucrose and 0.4% maltose. Growth (*A*) and viability (*B*) in the absence or the presence of compound 17 (seconeolitsine) at different concentrations were determined. Initial A_{620} values were 0.17 for pLS1R and 0.15 for pLS1R-topA. Initial viable values were 6.6×10^7 colony-forming units/ml for pLS1R and 3.2×10^7 colony-forming units/ml for pLS1R-topA.

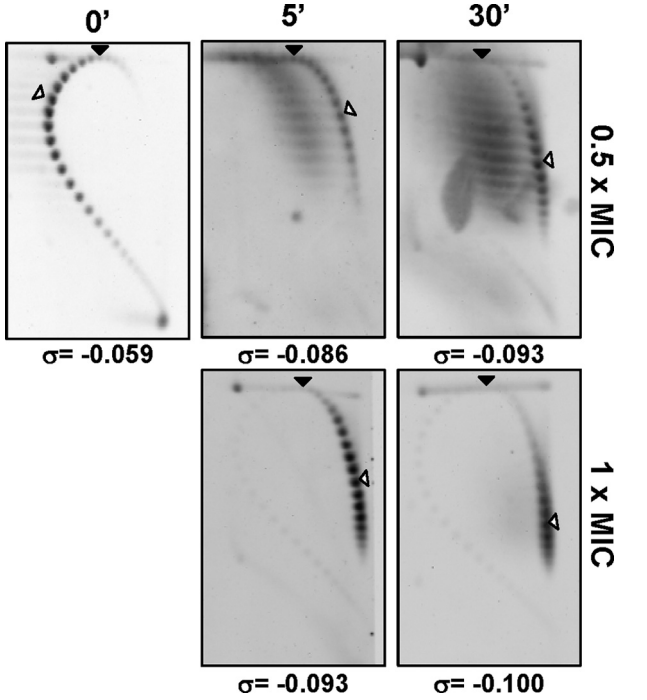

FIGURE 7. **Treatment with seconeolitsine causes hypernegative supercoiling in plasmid DNA.** An exponentially growing culture of R6 in AGCH carrying plasmid pLS1 was treated at $A_{620} = 0.4$ with seconeolitsine (compound 17) at 0.5× MIC and 1× MIC. Purified plasmid DNA from samples collected at 5 and 30 min after treatment was subjected to two-dimensional agarose gel electrophoresis in the presence of 5 μg/ml chloroquine in the first dimension and 15 μg/ml in the second dimension. It was previously determined that 15 μg/ml of chloroquine introduces 31 positive supercoils. A *black arrowhead* indicates the topoisomer that migrated with $\Delta Lk = 0$ in the second dimension. An *empty arrowhead* indicates the most abundant topoisomer. The corresponding supercoiling density (σ) is indicated below each autoradiogram.

(Fig. 9). Nevertheless this concentration was nearly 5-fold higher than that necessary to exert antibiotic activity.

DISCUSSION

Two main approaches can be used for the discovery of new antibiotics. The first approach is based on the screening of natural products for bacteria growth inhibition followed by the subsequent identification of the cellular target. The second uses the knowledge of the structure of essential enzyme targets to design different compounds. In this study both approaches have been successfully used to identify new alkaloid antibiotics. We have characterized for the first time the topoisomerase I enzyme of *S. pneumoniae* and completed the characterization of the DNA topoisomerase complement of this pathogen. Topoisomerase I is the unique DNA topoisomerase of type I in this bacterium and has enzymatic features similar to those found in Gram-negative bacteria, being able to relax negatively supercoiled DNA but not positively supercoiled DNA (Fig. 2).

A previous study carried out by Tse-Dinh's group (15) evaluated the capability of different compounds to inhibit topoisomerase I enzymes of Gram-negative bacteria (*E. coli* and *Yersinia pestis*). Among them, stephenanthrine (20–100 μM) was found to inhibit the relaxation activity of *E. coli* topoisomerase I via stabilization of the cleavage complex. However, this alkaloid did not affect bacterial growth at these concentrations, with MIC values of 60 and 100 μM for *Bacillus subtilis* (Gram-positive organism) and *E. coli*, respectively. These findings led us to test the activity of various boldine-derived compounds presenting a chemical structure similar to stephenanthrine. Among them, *N*-methyl-seconeolitsine and seconeolitsine displayed the most potent inhibitory activity of bacterial growth at concentrations within the range required for inhibition of the relaxation activity of *S. pneumoniae* topoisomerase I (Fig. 4 and Table 1). Moreover, these compounds also inhibited the growth of *S. pneumoniae* clinical isolates resistant to other chemically unrelated antibiotics used to treat pneumococcal infections (Table 1), including fluoroquinolones that target type II topoisomerases.

Attempts to obtain mutants resistant to the alkaloids were unsuccessful. These results suggest that the alteration of the single topoisomerase of type IA in *S. pneumoniae* could be

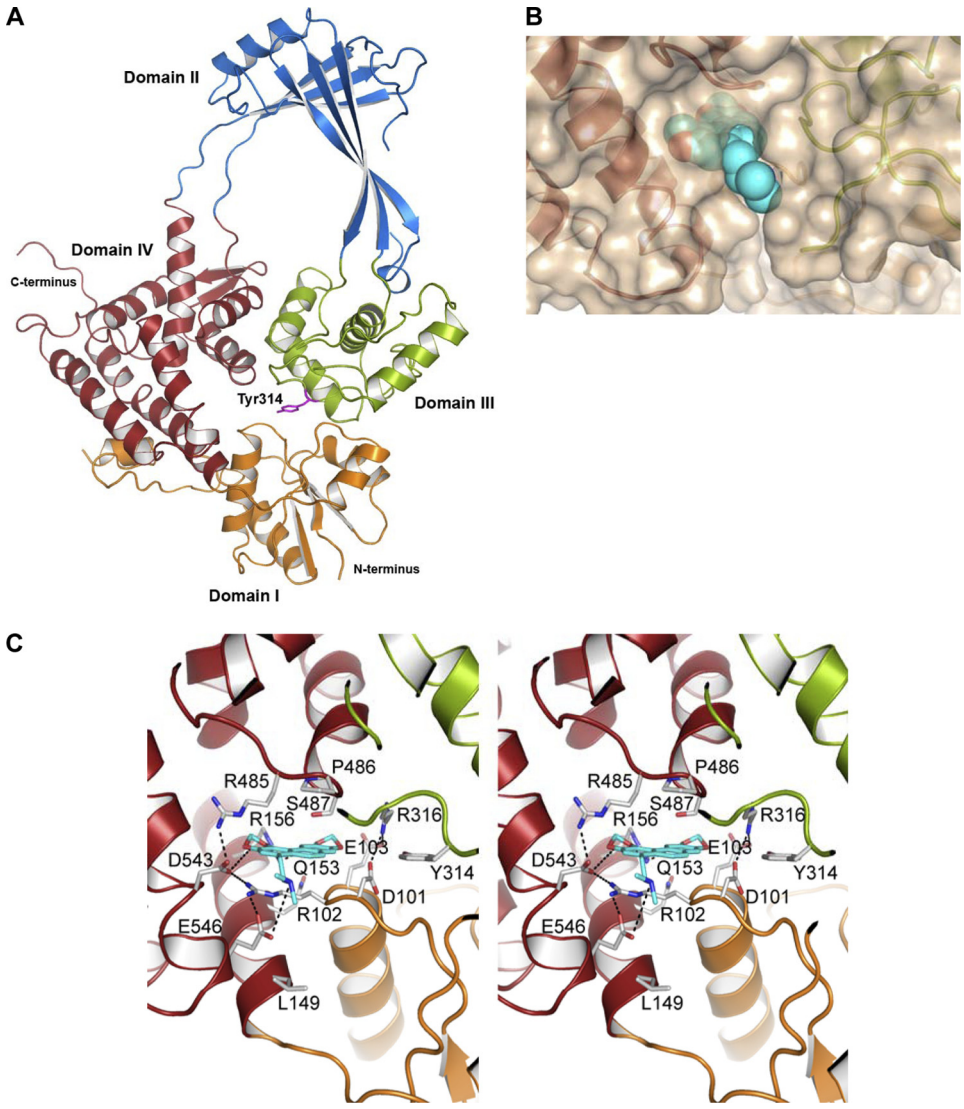

FIGURE 8. **Structural modeling of the interaction of *S. pneumoniae* topoisomerase I with alkaloid antibiotics.** *A*, overall structure of the 67-kDa fragment of *S. pneumoniae* TopA showing the four structural domains and the catalytic Tyr-314 residue (*magenta sticks*). *B*, *N*-methyl-seconeolitsine (represented as *blue spheres*) bound to the nucleotide-binding site of topoisomerase I. *C*, stereo view representation describing details of ligand recognition by topoisomerase I as obtained by docking calculations. The view shows the interactions between the nucleotide-binding site and *N*-methyl-seconeolitsine. The residues forming the binding site are drawn as *capped sticks*. Carbon atoms of the ligand are in *yellow*. Hydrogen bonds and salt bridge interactions are represented as *dashed lines*.

lethal, especially if the alteration would be at the DNA-binding site. In agreement, *E. coli* cells lacking their two type IA topoisomerases (TopA and TopB) are found to be nonviable (32).

Evidence for *in vivo* targeting of TopA by seconeolitsine was provided by the protection against growth inhibition when TopA was overproduced (Fig. 6). In fact, the increase in supercoiling of an internal plasmid in the presence of the alkaloid suggests an inhibition of TopA. This increase in supercoiling could be also caused by activation of gyrase or by inhibition of topoisomerase IV. However, these effects were not observed in the *in vitro* activities of purified pneumococcal gyrase and topoisomerase IV in the presence of *N*-methyl-seconeolitsine (data not shown). These results suggest that TopA is the intracellular target of compounds *N*-methyl-seconeolitsine and seconeolitsine and that these alkaloids might be useful in the treatment of infectious diseases caused by multidrug-resistant isolates. Although pharmacokinetic studies are required, our toxicological studies suggest that *N*-methyl-seconeolitsine and seconeolitsine (30 μM) did not affect human neutrophil viability (Fig. 8).

It has been proposed that the reaction cycle of topoisomerase I involves the opening and closing of the enzyme. For DNA to bind near the active site, the enzyme must adopt an open (or partially open) conformation (13). After the cleavage reaction takes place, the protein adopts an open conformation in which the protein forms a bridge between the two ends of the broken DNA strand. The opening of the enzyme would allow the entrance of another strand into the central hole. For the religation step to take place, the enzyme must bring the two ends of the broken strand together by bringing domains I and III together while keeping the passing strand inside the central hole of the enzyme. Clearly, different openings of the enzyme are required to display full activity. In this way, dock-

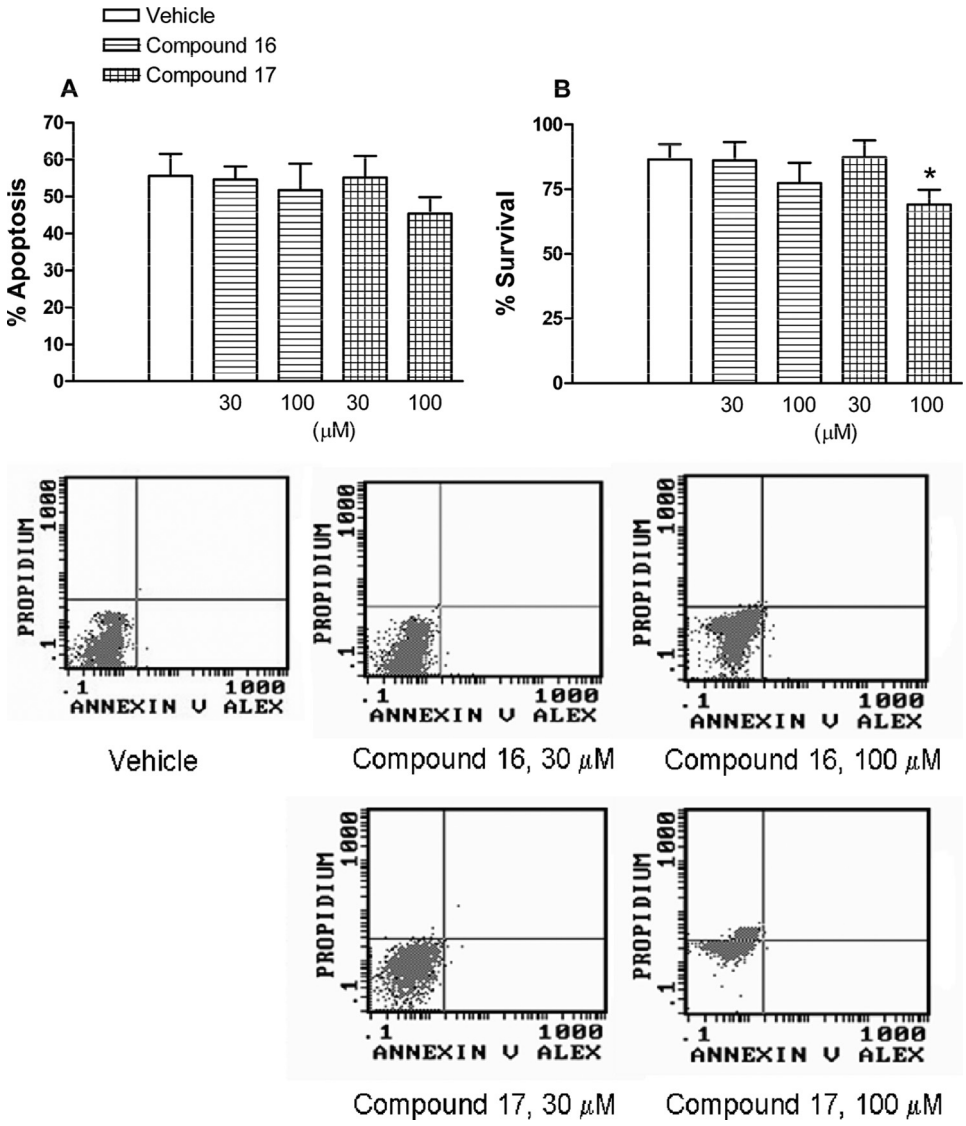

FIGURE 9. **Effect of compounds 16 and 17 on cell viability.** Percentage of apoptotic (*A*) and survival cells (*B*) after incubation with compounds 16 and 17 is shown. Early apoptotic cells were quantified as the percentage of total population of annexin V^+,PI^- cells, late apoptotic, and/or necrotic cells as annexin V^+ and PI^+, and viable nonapoptotic cells as annexin V^- and PI^- at 24 h of culture of human neutrophils. The columns are the means ± S.E. of 7–9 independent replicates. *, $p < 0.05$ compared with vehicle. Representative flow cytometry *panels* showing the effects of compounds 16 and 17 on human neutrophil apoptosis have been included.

ing calculations with alkaloids indicate that they can be accommodated at the nucleotide-binding site of the closed conformation of topoisomerase I. In this site alkaloids are in close contact with domains I, III, and IV (Fig. 7 and supplemental Fig. S2) and establish strong interactions (cation-π, hydrophobic, and polar interactions) with residues of the nucleotide-binding site. Boldine presents a more flexible structure without the extended π cloud of the seconeolitsine or *N*-methyl-seconeolitsine, therefore preventing a strong stabilization through cation-π interaction, as predicted for seconeolitsine or *N*-methyl-seconeolitsine. These strong interactions together with the fine fitting observed between the nucleotide-binding site and the alkaloid should block the opening mechanism required for topoisomerase I to be fully active. Therefore, avoidance of DNA binding may explain the strong inhibitory effect observed for these ligands. In agreement with that hypothesis, the inhibitory effect exerted by these alkaloids was enhanced prior to DNA binding. Thus, alkaloid-topoisomerase interactions seem to occur at the initial steps (*i.e.* in the closed conformation) and very likely in simultaneous interaction with the different domains involved in the opening mechanism of the enzyme.

Low concentrations of seconeolitsine and *N*-methyl-seconeolitsine seemed to activate the *in vitro* relaxation activity of human TOPO1, a prototype IB topoisomerase. However, the *in vitro* intercalation of these compounds in the DNA (Fig. 5*B*) would suggest that the alterations of TOPO1 activity could be attributed to this intercalation. In agreement, a similar effect was observed when the relaxing activity of TopA was tested in the presence of EtBr (Fig. 5*B*).

Higher alkaloid concentrations seemed to inhibit the *in vitro* activity of human TOPO1 without inducing apoptosis in human cells. In contrast, camptothecin, a selective inhibitor of TOPO1 used as antitumor drug, induces apoptosis. It binds

simultaneously both to the DNA and to topoisomerase I and stabilizes the cleavage complex formed by topoisomerase I-DNA and the drug. Then the collision of these cleavage complexes with replication forks induces double-stranded breaks that led to apoptosis (33). Therefore, it is likely either that alkaloid interaction with TOPO1 occurs before the single-stranded DNA cleavage is produced, because apoptosis was not detected, or that alkaloid did not interact with the enzyme.

In conclusion, in the present study we have isolated and purified a new antibiotic target from *S. pneumoniae*, topoisomerase I. Through the semi-synthesis of two new antibiotics, seconeolitsine and *N*-methyl-seconeolitsine, we have proven that topoisomerase I inhibition results in the blockade of bacteria growth without affecting the viability of human cells. These compounds did not cause any cytotoxic effect on human neutrophils at the concentrations required to exert antibiotic activity. Thus, seconeolitsine and *N*-methyl-seconeolitsine can be envisaged as two new therapeutic candidates for the treatment of *S. pneumoniae* infections resistant to other antibiotics and open a new scenario for designing more specific antibiotics targeting this pivotal enzyme.[3]

Acknowledgments—We thank Paloma Acebo, Mónica Amblar, and Pedro A. Lazo for critical reading of the manuscript. We also thank M. Calero for help with the ethidium bromide displacement assays.

REFERENCES

1. World Health Organization (2007) *Wkly. Epidemiol. Rec.* **82,** 93–104
2. Jacobs, M. R., Felmingham, D., Appelbaum, P. C., Grüneberg, R. N., and the Alexander Project Group (2003) *J. Antimicrob. Chemother.* **52,** 229–246
3. Mandell, L. A., Wunderink, R. G., Anzueto, A., Bartlett, J. G., Campbell, G. D., Dean, N. C., Dowell, S. F., File, T. M., Jr., Musher, D. M., Niederman, M. S., Torres, A., and Whitney, C. G. (2007) *Clin. Infect. Dis.* **44,** (Suppl. 2) S27–S72
4. de la Campa, A. G., Ardanuy, C., Balsalobre, L., Pérez-Trallero, E., Marimón, J. M., Fenoll, A., and Liñares, J. (2009) *Emerg. Infect. Dis.* **15,** 905–911
5. Champoux, J. J. (2001) *Annu. Rev. Biochem.* **70,** 369–413
6. Ferrándiz, M. J., Martín-Galiano, A. J., Schvartzman, J. B., and de la Campa, A. G. (2010) *Nucleic Acids Res.* **38,** 3570–3581
7. Drlica, K., Malik, M., Kerns, R. J., and Zhao, X. (2008) *Antimicrob. Agents Chemother.* **52,** 385–392
8. Muñoz, R., and de la Campa, A. G. (1996) *Antimicrob. Agents Chemother.* **40,** 2252–2257
9. Fernandez-Moreira, E., Balas, D., Gonzalez, I., and de la Campa, A. G. (2000) *Microb. Drug Resist.* **6,** 259–267
10. Caron, P. R., and Wang, J. C. (1994) *Adv. Pharmacol.* **29B,** 271–297
11. Sharma, A., Hanai, R., and Mondragón, A. (1994) *Structure* **2,** 767–777
12. Yu, L., Zhu, C. X., Tse-Dinh, Y. C., and Fesik, S. W. (1995) *Biochemistry* **34,** 7622–7628
13. Lima, C. D., Wang, J. C., and Mondragón, A. (1994) *Nature* **367,** 138–146
14. Feinberg, H., Lima, C. D., and Mondragón,A. (1999) *Nat. Struct. Biol.* **6,** 918–922
15. Cheng, B., Liu, I. F., and Tse-Dinh, Y. C. (2007) *J. Antimicrob. Chemother.* **59,** 640–645
16. Lacks, S. A., Lopez, P., Greenberg, B., and Espinosa, M. (1986) *J. Mol. Biol.* **192,** 753–765
17. National Committee for Clinical Laboratory Standards (2004) *Performance Standards for Antimicrobial Susceptibility Testing: Approved Standard M100-S14,* National Committee for Clinical Laboratory Standards, Wayne, PA
18. Nieto, C., Fernández de Palencia, P., López, P., and Espinosa, M. (2000) *Plasmid* **43,** 205–213
19. Mateo, T., Naim Abu Nabah, Y., Losada, M., Estellés, R., Company, C., Bedrina, B., Cerdá-Nicolás, J. M., Poole, S., Jose, P. J., Cortijo, J., Morcillo, E. J., and Sanz, M. J. (2007) *Blood* **110,** 1895–1902
20. Martin, M. C., Dransfield, I., Haslett, C., and Rossi, A. G. (2001) *J. Biol. Chem.* **276,** 45041–45050
21. Jones, T. A., Zou, J. Y., Cowan, S. W., and Kjeldgaard, M. (1991) *Acta Crystallogr. A* **47,** 110–119
22. Brünger, A. T., Adams, P. D., Clore, G. M., DeLano, W. L., Gros, P., and Grosse-Kunstleve, R. W., Jiang, J. S., Kuszewski, J., Nilges, M., Pannu, N. S., Read, R. J., Rice, L. M., Simonson, T., and Warren, G. L. (1998) *Acta Crystallogr. D Biol. Crystallogr.* **54,** 905–921
23. Laskowski, R. A., Moss, D. S., and Thornton, J. M. (1993) *J. Mol. Biol.* **231,** 1049–1067
24. Schüttelkopf, A. W., and van Aalten, D. M. (2004) *Acta Crystallogr. D Biol. Crystallogr.* **60,** 1355–1363
25. Macrae, C. F., Bruno, I. J., Chisholm, J. A., Edgington, P. R., McCabe, P., Pidcock, E., Rodríguez-Monge, L., Taylor, R., van de Streek, J., and Wood, P. A. (2008) *J. Appl. Crystallogr.* **41,** 466–470
26. Verdonk, M. L., Cole, J. C., Hartshorn, M. J., Murray, C. W., and Taylor, R. D. (2003) *Proteins* **52,** 609–623
27. Hoskins, J., Alborn, W. E., Jr., Arnold, J., Blaszczak, L. C., Burgett, S., DeHoff, B. S., Estrem, S. T., Fritz, L., Fu, D. J., Fuller, W., Geringer, C., Gilmour, R., Glass, J. S., Khoja, H., Kraft, A. R., Lagace, R. E., LeBlanc, D. J., Lee, L. N., Lefkowitz, E. J., Lu, J., Matsushima, P., McAhren, S. M., McHenney, M., McLeaster, K., Mundy, C. W., Nicas, T. I., Norris, F. H., O'Gara, M., Peery, R. B., Robertson, G. T., Rockey, P., Sun, P. M., Winkler, M. E., Yang, Y., Young-Bellido, M., Zhao, G., Zook, C. A., Baltz, R. H., Jaskunas, S. R., Rosteck, P. R., Jr., Skatrud, P. L., and Glass, J. I. (2001) *J. Bacteriol.* **183,** 5709–5717
28. Keller, W. (1975) *Proc. Natl. Acad. Sci. U.S.A.* **72,** 2550–2554
29. Depew, D. E., and Wang, J. C. (1975) *Proc. Natl. Acad. Sci. U.S.A.* **72,** 4275–4279
30. Martín-Parras, L., Lucas, I., Martínez-Robles, M. L., Hernández, P., Krimer, D. B., Hyrien, O., and Schvartzman, J. B. (1998) *Nucleic Acids Res.* **26,** 3424–3432
31. Milián, L., Estellés, R., Abarca, B., Ballesteros, R., Sanz, M. J., and Blázquez, M. A. (2004) *Chem. Pharm. Bull.* **52,** 696–699
32. Stupina, V. A., and Wang, J. C. (2005) *J. Biol. Chem.* **280,** 355–360
33. Pommier, Y. (2006) *Nat. Rev. Cancer* **6,** 789–802

[3] García, M. T., Blázquez, M. A., and de la Campa, A. G. (December 18, 2009) *Use of Seconeolitsine and N-methyl-seconeolitsine for the Manufacture of Medical Products*. Patent pending, P200931186.